Plasma Chemistry and Kinetics in Low Pressure Discharges: The significance of metastable states

Jón Tómas Guðmundsson[1,2]

[1] Science Institute, University of Iceland, Reykjavik, Iceland
[2]Department of Space and Plasma Physics, School of Electrical Engineering, KTH Royal Institute of Technology, SE-100 44, Stockholm, Sweden

tumi@hi.is

Linköpings Universitet, Linköping, Sweden
January 21., 2016

Outline

- A. Global (volume averaged) chemistry models
  - A.1 The argon discharge
  - A.2 The chlorine discharge
    - oxygen dilution
- B. 1D particle-in-cell/Monte Carlo collision simulation
  - B.1 Capacitively Coupled Oxygen Discharge at 13.56 MHz – Voltage Source – pressure dependence
  - B.2. Capacitively Coupled Chlorine Discharge – dual frequency 27.12 MHz and 2 MHz – Current Source
- C. Summary

A. Global (volume averaged) chemistry models

Global (volume averaged) chemistry models

- The main idea of a global model is to generate a model that encompasses a large number of reactions in order to model a processing plasma with a limited computing power by neglecting the complexity which arises when spatial variations are considered
- Thus the model does not describe spatial distribution but captures scalings of plasma parameters with control parameters
- The model allows us to investigate various phenomena, such as the effects of excited species, negative ions and particular reactions on the overall discharge

Global (volume averaged) chemistry models

- All densities are assumed to be volume averaged
- For an electropositive discharge the positive-ion densities are assumed to have a uniform profile throughout the discharge except near the wall, where the density is assumed to drop sharply to a sheath-edge density $n_{\rm is}$
- The electron energy distribution function (EEDF) is assumed (usually Maxwellian)
- The ion and neutral temperature have to be assumed

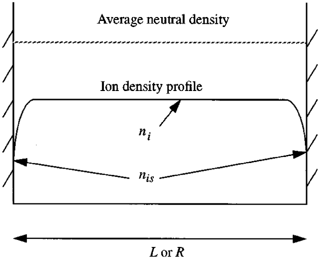

Lee and Lieberman *JVSTA*, **13** (1995) 368

A.1 Global (volume averaged) chemistry models – argon discharge

Argon discharge – electron - neutral collisions

- In its simplest form argon discharge consists of

$$\mathrm{e, Ar, Ar^{+}, Ar^{*}}$$

- There are electron-atom collisions

$$\mathrm{e + Ar \longrightarrow Ar^{+} + 2e} \qquad \text{(ionization)}$$

$$\mathrm{e + Ar \longrightarrow Ar^{*} + e \longrightarrow Ar + e + photon} \qquad \text{(excitation)}$$

$$\mathrm{e + Ar \longrightarrow Ar + e} \qquad \text{(elastic scattering)}$$

- The reactions are described by **rate coefficients**

$$k(\mathrm{T_e}) = \langle \sigma(v_\mathrm{R}) v_\mathrm{R} \rangle$$

where $\sigma(v_\mathrm{R})$ is the cross section and v_R is the relative velocity of colliding particles

Argon discharge – electron - neutral collisions

- The electron energy distribution function (EEDF) is usually assumed to be Maxwellian
- We can also assume a general electron energy distribution

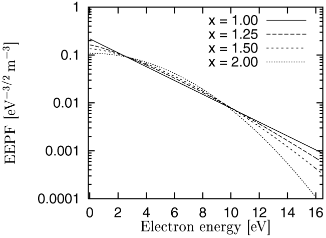

$$g_{\rm e}(\mathcal{E}) = c_1 \mathcal{E}^{1/2} \exp\left(-c_2 \mathcal{E}^x\right)$$

$$c_1 = \frac{1}{\langle \mathcal{E} \rangle^{3/2}} \frac{[\Gamma(\xi_2)^{3/2}]}{[\Gamma(\xi_1)^{5/2}]} \quad \text{and} \quad c_2 = \frac{1}{\langle \mathcal{E} \rangle^x} \frac{[\Gamma(\xi_2)]}{[\Gamma(\xi_1)]^x}$$

where $\xi_1 = 3/2x$ and $\xi_2 = 5/2x$

$$g_{\rm p}(\mathcal{E}) = \frac{g_{\rm e}(\mathcal{E})}{\mathcal{E}^{1/2}}$$

- Here $x = 1$ and $x = 2$ correspond to Maxwellian and Druyvesteyn electron energy distributions, repectively

Gudmundsson *PSST*, **10** (2001) 76

Argon discharge – ion - neutral collisions

- Argon ions collide with argon atoms

$$\mathrm{Ar}^+ + \mathrm{Ar} \longrightarrow \mathrm{Ar}^+ + \mathrm{Ar} \qquad \text{(elastic scattering)}$$

$$\mathrm{Ar}^+ + \mathrm{Ar} \longrightarrow \mathrm{Ar} + \mathrm{Ar}^+ \qquad \text{(charge transfer)}$$

- The total cross section for ions at room temperature

$$\sigma_{\mathrm{i}} \approx 10^{-18}\ \mathrm{m}^2$$

- The ion-neutral mean free path – the distance an ion travels before colliding is

$$\lambda_{\mathrm{i}} = \frac{1}{n_{\mathrm{g}}\sigma_{\mathrm{i}}} = \lambda_{\mathrm{i}}\ [\mathrm{cm}] = \frac{1}{330\ p\ [\mathrm{Torr}]}$$

where n_{g} is the neutral gas density – $\lambda_{\mathrm{i}} \approx 1$ cm at 3 mTorr

Argon discharge – Energy loss processes

- There are three energy loss processes:
  - **Collisional energy** $\mathcal{E}_c$ lost per electron-ion pair created

$$\mathcal{E}_c(T_e) = \mathcal{E}_{iz} + \sum_{i=1}^{n} \frac{k_{ex,i}}{k_{iz}} \mathcal{E}_{ex,i} + \frac{k_{el}}{k_{iz}} \frac{3m_e}{M} T_e$$

  - **Electron kinetic energy** lost to walls

$$\mathcal{E}_e = 2T_e \quad \text{if Maxwellian EEDF}$$

  - **Ion kinetic energy** lost to walls

$$\mathcal{E}_i \approx \bar{V}_s$$

    or mainly the dc potential across the sheath

- The total energy lost per electron-ion pair lost to walls

$$\mathcal{E}_T = \mathcal{E}_c + \mathcal{E}_e + \mathcal{E}_i$$

Argon discharge – Collisional energy losses

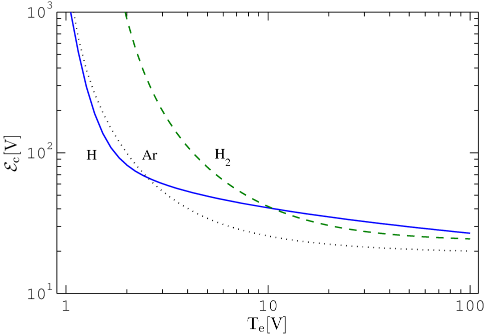

- The collisional energy loss per electron-ion pair created for argon, hydrogen atoms and hydrogen molecules assuming Maxwellian EEDF

Hjartarson et al., *Plasma Sources Sci. Technol.*, **19** 065009 (2010)

Argon discharge – Ion loss

- Ions are lost at the **Bohm velocity** at the plasma-sheath edge

$$u_{\rm i} = u_{\rm B} = \left(\frac{k_{\rm B} T_{\rm e}}{M}\right)^{1/2}$$

assuming Maxwellian energy distribution or more generally

$$v_{\rm i} = \langle \mathcal{E} \rangle^{1/2} \left(\frac{2}{M}\right)^{1/2} \frac{[\Gamma(\xi_1)]}{[\Gamma(\xi_2)\Gamma(\xi_3)]^{1/2}}$$

where $\xi_1 = 3/2x$, $\xi_2 = 5/2x$ and $\xi_3 = 1/2x$

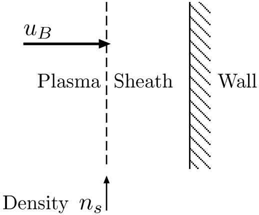

Argon discharge – Diffusion

- A low pressure (< 100 mTorr in argon) the plasma density profile is relatively flat in the center and falls sharply near the sheath edge
- Ion and electron loss to the wall is

$$\Gamma_{\rm wall} = n_{\rm s} u_{\rm B} \equiv h_\ell n_0 u_{\rm B}$$

- The **edge-to-center density ratio** is

$$h_\ell \equiv \frac{n_{\rm s}}{n_0} \approx \frac{0.86}{(3 + \ell/2\lambda_{\rm i})^{1/2}}$$

where $\lambda_{\rm i}$ is the ion-neutral mean free path

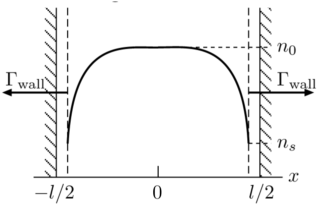

Argon discharge – Cylindrical discharge

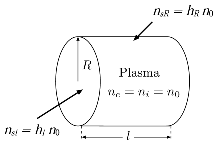

- Loss fluxes to the axial and radial walls are

$$\Gamma_{\rm axial} = h_\ell n_0 u_{\rm B} \quad \text{and} \quad \Gamma_{\rm radial} = h_{\rm R} n_0 u_{\rm B}$$

and the edge-to-center density ratios are

$$h_\ell \approx \frac{0.86}{(3 + \ell/2\lambda_{\rm i})^{1/2}} \quad \text{and} \quad h_{\rm R} \approx \frac{0.8}{(4 + R/\lambda_{\rm i})^{1/2}}$$

Godyak, *Soviet Radio Frequency Discharge Research* (1986)

Argon discharge – Cylindrical discharge

- At high pressure

$$\ell \frac{T_{\rm i}}{T_{\rm e}} \geq \lambda_{\rm i}$$

  a constant diffusion model is more appropriate

$$h_\ell \approx \frac{\pi D_{\rm a}}{\ell u_{\rm B}}$$

- These regimes can be joined heuristically giving

$$h_\ell \approx \frac{0.86}{\left[3 + \ell/2\lambda_{\rm i} + (0.86 R u_{\rm B}/\pi D_{\rm a})^2\right]^{1/2}}$$

$$h_{\rm R} \approx \frac{0.8}{\left[4 + R/\lambda_{\rm i} + (0.8 R u_{\rm B}/\chi_{01} {\rm J}_1(\chi_{01}) D_{\rm a})^2\right]^{1/2}}$$

Lee and Lieberman *J. Vac. Sci. Technol. A*, **13** (1995) 368

Lieberman and Lichtenberg, *Principles of Plasma Discharges*, 2nd ed., John Wiley & Sons 2005

Argon discharge – Particle balance

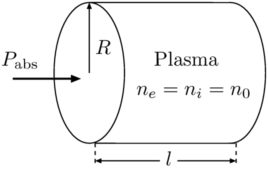

- We assume a uniform cylindrical plasma and the absorbed power is $P_{\rm abs}$
- Particle balance

$$\underbrace{n_{\rm g} n_0 k_{\rm iz} R^2 \ell}_{\text{ionization in the bulk plasma}} = \underbrace{(2\pi R^2 h_\ell n_0 + 2\pi R \ell h_{\rm R} n_0) u_{\rm B}}_{\text{ion loss to walls}}$$

Argon discharge – Particle balance

- Rearrange to obtain

$$\frac{k_{\rm iz}(T_{\rm e})}{u_{\rm B}(T_{\rm e})} = \frac{1}{n_{\rm g} d_{\rm eff}}$$

where

$$d_{\rm eff} = \frac{1}{2}\frac{R\ell}{Rh_\ell + \ell h_R}$$

is an effective plasma size

- So given $n_{\rm g}$ (pressure) and $d_{\rm eff}$ (pressure,dimensions) we know $T_{\rm e}$
- The electron temperature is generally in the range 2 – 5 V

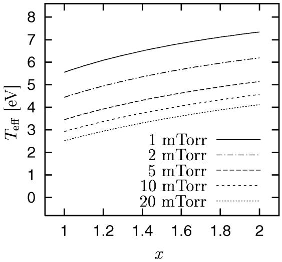

$R = 15.24$ cm

$\ell = 7.6$ cm

Gudmundsson *PSST*, **10** (2001) 76

Argon discharge – Power balance

- The power balance is

$$\underbrace{P_{\mathrm{abs}}}_{\text{power in}} = \underbrace{(h_\ell n_0 2\pi R^2 + h_{\mathrm{R}} n_0 2\pi R\ell) u_{\mathrm{B}} e\mathcal{E}_{\mathrm{T}}}_{\text{power lost}}$$

- Solve for particle density

$$n_0 = \frac{P_{\mathrm{abs}}}{A_{\mathrm{eff}} u_{\mathrm{B}} e\mathcal{E}_{\mathrm{T}}}$$

where

$$A_{\mathrm{eff}} = 2\pi R^2 h_\ell + 2\pi R\ell h_{\mathrm{R}}$$

is an effective area for particle loss

- Assume low voltage sheaths at all surfaces

$$\mathcal{E}_{\mathrm{T}} = \mathcal{E}_{\mathrm{c}} + \mathcal{E}_{\mathrm{e}} + \mathcal{E}_{\mathrm{i}} = \mathcal{E}_{\mathrm{c}}(\mathrm{T_e}) + 2\mathrm{T_e} + 5.2\mathrm{T_e}$$

Argon discharge – Power and particle balance

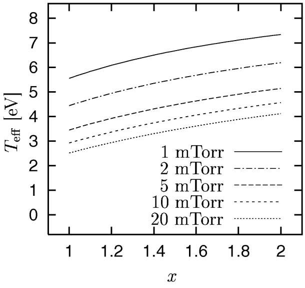

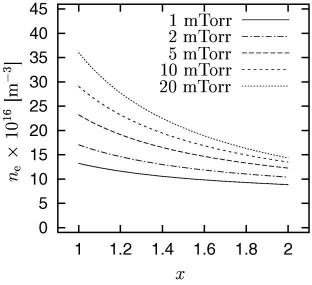

- Particle balance gives the electron temperature
  - only depends on the neutral gas pressure and system dimensions
- Power balance gives the plasma density
  - Once we know the electron temperature

Gudmundsson *Plasma Sources Sci. Technol.*, **10** (2001) 76

A.2 Global (volume averaged) chemistry models – chlorine

The chlorine discharge

- Chlorine is an electronegative diatomic gas that is widely used in plasma etching of both semiconductors and metals, in particular poly-silicon gate and aluminum interconnects
- Chlorine atoms are believed to be the primary reactant in plasma etching
- The chlorine molecule has
  - a low dissociation energy (2.5 eV)
  - a near-zero threshold energy for dissociative attachment
- All electronic excitations of the molecule appear to be dissociative, and no metastable molecular states are of importance

The global (volume averaged) model

- A steady state global (volume averaged) model was developed for the chlorine discharge
- The following species are included
  - electrons
  - the ground state chlorine molecule $Cl_2(X\,^1\Sigma_g^+, v = 0)$,
  - the vibrationally excited ground state chlorine molecules $Cl_2(X\,^1\Sigma_g^+, v = 1-3)$
  - the ground state chlorine atom $Cl(3p^5\,^2P)$
  - the negative chlorine ion Cl^-
  - the positive chlorine ions Cl^+ and Cl_2^+
- The content of the chamber is assumed to be nearly spatially uniform and the power is deposited uniformly into the plasma bulk

Thorsteinsson and Gudmundsson, *Plasma Sources Sci. Technol.*, **19** (2010) 015001

The global (volume averaged) model

- The particle balance equation for a species X is given

$$\frac{\mathrm{d}n^{(X)}}{\mathrm{d}t} = 0 = \sum_i R^{(X)}_{\mathrm{Generation},i} - \sum_i R^{(X)}_{\mathrm{Loss},i}$$

  where $R^{(X)}_{\mathrm{Generation},i}$ and $R^{(X)}_{\mathrm{Loss},i}$, respectively, are the reaction rates of the various generation and loss processes of the species X

- The power balance equation, which equates the absorbed power P_{abs} to power losses due to elastic and inelastic collisions and losses due to charged particle flow to the walls is given as

$$\frac{1}{V}\left[P_{\mathrm{abs}} - eVn_{\mathrm{e}}\sum_\alpha n^{(\alpha)}\mathcal{E}_{\mathrm{c}}^{(\alpha)}k_{\mathrm{iz}}^{(\alpha)} - eu_{\mathrm{B0}}n_{\mathrm{i}}A_{\mathrm{eff}}(\mathcal{E}_{\mathrm{i}} + \mathcal{E}_{\mathrm{e}})\right] = 0$$

The global (volume averaged) model

- For the edge-to-center positive ion density ratio we use

$$h_\ell \simeq \left[\left(\frac{0.86}{(3+\eta L/2\lambda_{\rm i})^{1/2}}\frac{1}{1+\alpha_0}\right)^2 + h_{\rm c}^2\right]^{1/2}$$

$$h_{\rm R} \simeq \left[\left(\frac{0.8}{(4+\eta R/\lambda_{\rm i})^{1/2}}\frac{1}{1+\alpha_0}\right)^2 + h_{\rm c}^2\right]^{1/2}$$

where $\alpha_0 \approx (3/2)\alpha$ is the central electronegativity,
$\eta = 2T_+/(T_+ + T_-)$ and

$$h_{\rm c} \simeq \left[\gamma_-^{1/2} + \gamma_+^{1/2}[n_*^{1/2}n_+/n_-^{3/2}]\right]^{-1} \quad \text{and} \quad n_* = \frac{15}{56}\frac{\eta^2}{k_{\rm rec}\lambda_{\rm i}}v_{\rm i}$$

is based on a one-region flat topped electronegative profile

$$\gamma_- = {\rm T_e}/{\rm T_-} \quad \text{and} \quad \gamma_+ = {\rm T_e}/{\rm T_+}$$

Kim et al., J. Vac. Sci. Technol. A, **24** (2006) 2025

The global (volume averaged) model

- The diffusional losses of the neutral chlorine atoms to the reactor walls are given by

$$k_{\mathrm{Cl,wall}} = \left[\frac{\Lambda_{\mathrm{Cl}}^2}{D_{\mathrm{Cl}}} + \frac{2V(2-\gamma_{\mathrm{rec}})}{A v_{\mathrm{Cl}} \gamma_{\mathrm{rec}}} \right]^{-1} \quad \mathrm{s}^{-1}$$

  - D_{Cl} is the diffusion coefficient for neutral chlorine atoms
  - $v_{\mathrm{Cl}} = (8eT_{\mathrm{g}}/\pi m_{\mathrm{Cl}})^{1/2}$ is the mean Cl velocity
  - γ_{rec} is the wall recombination coefficient for neutral chlorine atoms on the wall surface
  - Λ_{Cl} is the effective diffusion length of neutral chlorine atoms

$$\Lambda_{\mathrm{Cl}} = \left[\left(\frac{\pi}{L}\right)^2 + \left(\frac{2.405}{R}\right)^2 \right]^{-1/2}$$

- The wall recombination coefficient γ_{rec} is one of the most important parameters in chlorine discharge modelling

A.2.1 Model parameters

Surface recombination

- The wall recombination probability, $\gamma_{\rm rec}$, is a very important quantity in all low pressure molecular discharges
- We use the wall recombination coefficient measured by Stafford et al. (2009) for stainless steel

Guha et al. J. Appl. Phys., **103** (2008) 013306

Stafford et al. J. Phys. D: Appl. Phys. **42** (2009) 055206

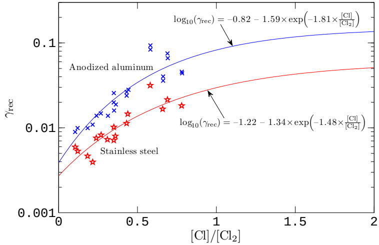

A fit to the measured data is for anodized aluminum

$$\log_{10}(\gamma_{\rm rec}) = -0.82 - 1.59 \exp\left(-1.81 \times \frac{[{\rm Cl}]}{[{\rm Cl_2}]}\right)$$

and for stainless steel

$$\log_{10}(\gamma_{\rm rec}) = -1.22 - 1.34 \exp\left(-1.48 \times \frac{[{\rm Cl}]}{[{\rm Cl_2}]}\right)$$

Gas temperature

- Donnelly and Malyshev (2000) found that the neutral chlorine gas temperature was between 300 and 1250 K, increasing with power and pressure up to 1000 W and 20 mTorr

Donnelly and Malyshev, Appl. Phys. Lett. **77** 2467 (2000)

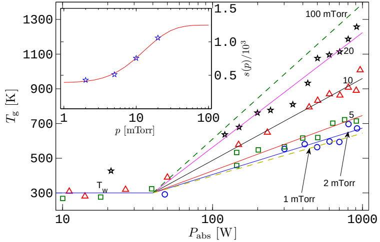

A fit through the measured data gives

$$T_g(P_{abs}, p) = 300 + s(p)\frac{\log_{10}(P_{abs}/40)}{\log_{10}(40)}$$

where

$$s(p) = 1250\,(1 - e^{-0.091\times p}) + 400\,e^{-0.337\times p}$$

A.2.2 Comparison with experiments

Comparison with experiments

- Densities of neutral Cl atoms and electrons versus power
- The agreement with the measured electron density is excellent
- The calculated density of atomic chlorine is in a very good agreement with the measured data at both 1 and 10 mTorr

Malyshev and Donnelly, J. Appl. Phys. **88** (2000) 6207

Malyshev and Donnelly, J. Appl. Phys. **90** (2001) 1130

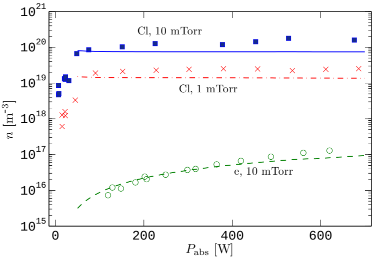

- inductively coupled cylindrical stainless steel chamber
- $L = 20$ cm and $R = 18.5$ cm

A.2.3 Particle densities

Particle densities

- Atomic chlorine Cl is the dominant particle at low pressure, but the chlorine molecule Cl_2 has a larger density above 20 mTorr
- The density of the atomic ion Cl^+ is always much smaller than the Cl_2^+ density, decreasing with increasing pressure
- a cylindrical stainless steel chamber radius $R = 18.5$ cm and length $L = 20$ cm

  $P_{abs} = 323$ W

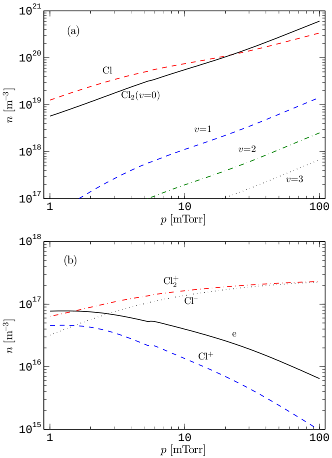

Thorsteinsson and Gudmundsson, *Plasma Sources Sci. Technol.*, **19** (2010) 015001

Creation and destruction of Cl atoms

- Electron impact dissociation

$$e + Cl_2 \longrightarrow Cl + Cl + e$$

is the most important channel for creation of Cl atoms

- Recombination at the wall

$$Cl \longrightarrow \frac{1}{2}Cl_2$$

accounts for 40 – 93 % and is the most important channel for Cl atom loss

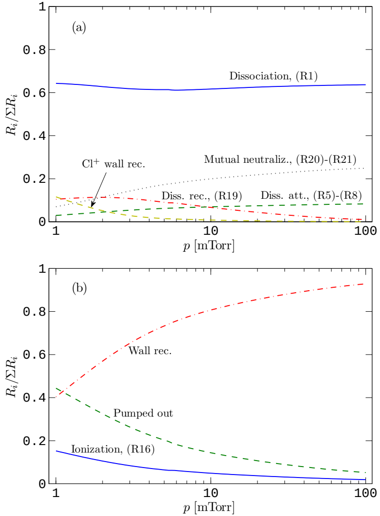

Creation and destruction of Cl^- ions

- The production of Cl^--ions is only due to dissociative electron attachment

$$e + Cl_2 \longrightarrow Cl + Cl^-$$

- Vibrational levels contribute at most 14 % at 100 mTorr
- Cl^- ions are primarily lost by mutual neutralization

$$Cl^- + Cl_2^+ \longrightarrow Cl + Cl + Cl$$

$$Cl^- + Cl^+ \longrightarrow Cl + Cl$$

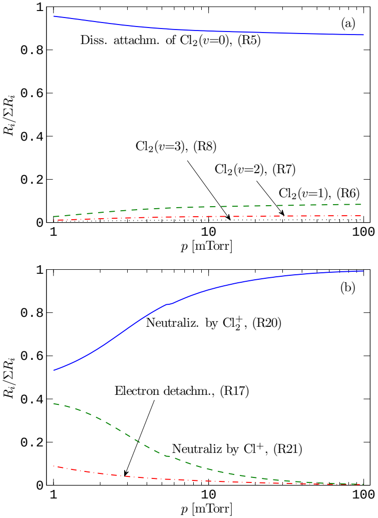

A.2.4 Sensitivity analysis

Sensitivity analysis – EEDF

- The discharge pressure was 10 mTorr and the absorbed power 323 W
- We allow the electron energy distribution function to vary according to the general distribution function

$$g_{\mathrm{e}}(\mathcal{E}) = c_1 \mathcal{E}^{1/2} \exp(-c_2 \mathcal{E}^x)$$

where the coefficients c_1 and c_2 depend on the energy $\mathcal{E}$ and the distribution parameter x

	$[\mathrm{Cl}]/n_{\mathrm{g}}$	$[\mathrm{Cl}^+]/n_+$	α	$\mathrm{T_e}$	n_{e}
x: 1 – 2	$\downarrow$ 1.01	$\downarrow$ 1.40	$\uparrow$ 1.34	$\uparrow$ 1.43	$\downarrow$ 1.65

Gudmundsson et al., *Vacuum*, **86** (2012) 808

Sensitivity analysis – $\gamma_{\rm rec}$

	$[\mathrm{Cl}]/n_{\rm g}$	$[\mathrm{Cl}^+]/n_+$	α	$\mathrm{T_e}$	$n_{\rm e}$
$\gamma_{\rm rec}$: 10^{-4} – 1	$\downarrow$ 5.75	$\downarrow$ 34.6	$\uparrow$ 4.25	$\uparrow$ 1.13	$\downarrow$ 1.59

- The wall recombination coefficient $\gamma_{\rm rec}$ determines the rate coefficient for recombination of neutrals on the wall
- However, varying $\gamma_{\rm rec}$ has a much larger effect on the atomic ion fraction than on the dissociation fraction

A.2.5 Oxygen dilution

Oxygen dilution – Particle densities

- The Cl^+ density decreases with increased oxygen dilution
- The chlorine-oxide molecule ClO and its ion ClO^+ peak when Cl_2 and O_2 flowrates are roughly equal
- The $O_2(a^1\Delta_g)$ density is about 9 – 10 % of the total O_2 density
- The electron density increases about 30 % between pure chlorine and pure oxygen discharge

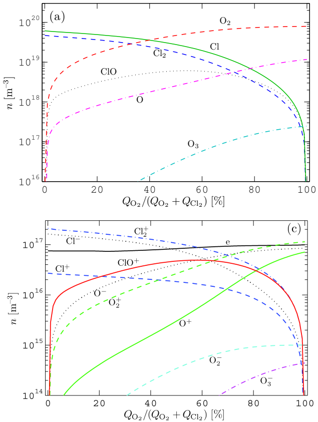

A cylindrical stainless steel chamber
L = 10 cm and R = 10 cm
p = 10 mTorr and P_{abs} = 500 W

Oxygen dilution – Particle densities

- The total rate for creation and loss of ClO molecules is at maximum when the oxygen content is 65%.
- Wall recombination of Cl molecules, is the dominating pathway for creation of ClO molecules
- The bulk processes and recombination of ClO^+ ions at the wall account for roughly 33–43% of the total rate for ClO creation, combined

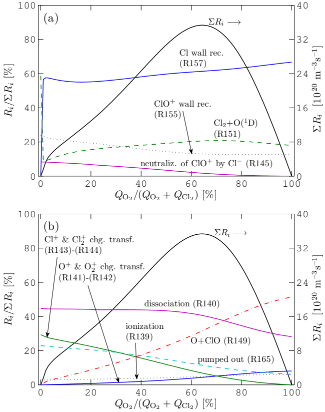

Thorsteinsson and Gudmundsson, *Plasma Sources Sci. Technol.*, **19** 055008 (2010)

A.3 Summary

Summary

- A global model of Cl_2, Cl_2/Ar and Cl_2/O_2 discharges has been developed
- The chlorine discharge remains highly dissociated in all conditions, being over 20 % at the lowest power and highest pressure explored
- Cl^- ions are essentially entirely produced in dissociative attachment of electrons to Cl_2 and lost to mutual neutralization with Cl^+ and Cl_2^+
- The effect of vibrationally excited chlorine molecules $Cl_2(v > 0)$ is not great, at most increasing the Cl^- production by about 14 %
- The Cl^+ density increases with increased argon dilution but decreases with increased oxygen dilution
- The ClO molecule is mainly created by recombination at the discharge wall

B. 1D particle-in-cell/Monte Carlo collision simulation

Outline

- The 1D particle-in-cell/Monte Carlo collision simulation
  - The oxygen discharge
    - Capacitively Coupled Oxygen Discharge at 13.56 MHz – Voltage Source – pressure dependence
  - The chlorine discharge
    - Capacitively Coupled Chlorine Discharge – dual frequency 27.12 MHz and 2 MHz – Current Source
  - Summary

The 1D particle-in-cell/Monte Carlo collision simulation

The oopd1 1d-3v PIC/MCC code

- In particle-in-cell simulation the plasma is represented as a collection of macroparticles
- Each macroparticle is a charged “cloud” representing many real charged particles
- Each macroparticle has the same charge-to-mass ratio (q/m) as the real charged particle
- Equations of motion are solved for each macroparticle
- The electric and magnetic fields are calculated self-consistently using charge densities and currents produced by the macroparticles

The oopd1 1d-3v PIC/MCC code

- We use the `oopd1` (objective oriented plasma device for one dimension) code to simulate the discharge
- The `oopd1` code was originally developed at the Plasma Theory and Simulation Group at UC Berkeley
- It has 1 dimension in space and 3 velocity components for particles (1d-3v)
- The `oopd1` code is supposed to replace the widely used `xpdx1` series (`xpdp1`, `xpdc1` and `xpds1`)
- It is developed to simulate various types of plasmas, including processing discharges, accelerators and beams
  - Modular structure
  - Includes relativistic kinematics
  - Particles can have different weights

Gudmundsson et al., *Plasma Sources Sci. Technol.*, **22** 035011 (2013)

B.1. The oxygen discharge

The oxygen discharge

- We consider a discharge that consists of:
  - electrons
  - the ground state oxygen molecule $O_2(X^3\Sigma_g^-)$
  - the metastable oxygen molecule $O_2(a^1\Delta_g)$
  - the metastable oxygen molecule $O_2(b^1\Sigma_g)$
  - the ground state oxygen atom $O(^3P)$
  - the metastable oxygen atom $O(^1D)$
  - the negative oxygen ion O^-
  - the positive oxygen ions O^+ and O_2^+
- We apply a global model[1] beforehand to calculate the partial pressure of the various neutrals

[1] Thorsteinsson and Gudmundsson, *Plasma Sources Sci. Technol.*, **19** 055008 (2010)

The oxygen discharge

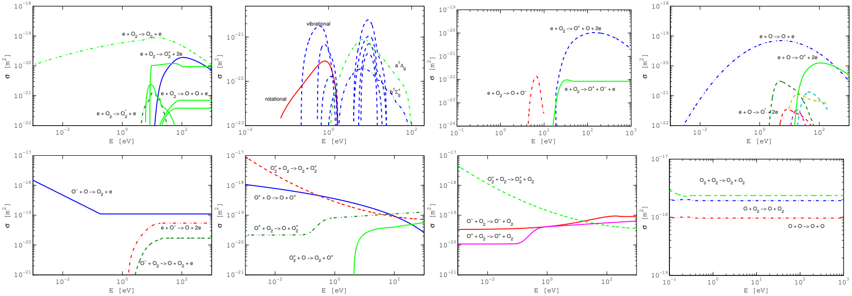

- The reaction set for the oxygen is comprehensive and for this study includes 67 reactions

Gudmundsson et al., *Plasma Sources Sci. Technol.*, **22** 035011 (2013), and **24** 035016 (2015)

B. 1. 1. Capacitively Coupled Oxygen Discharge at 13.56 MHz – pressure dependence – including $O_2(a^1\Delta_g)$

Capacitively Coupled Oxygen Discharge at 13.56 MHz

- We apply a voltage source with a single frequency

$$V(t) = V_{\mathrm{rf}} \sin(2\pi f t)$$

- The electrodes are circular with a diameter of 14.36 cm
- The gap between the electrodes is 4.5 cm
- We set V_{rf} = 222 V and f = 13.56 MHz
- The neutrals (O_2 and O) are treated as background gas at T_{g} = 300 K with a Maxwellian distribution
- The dissociation fraction and the metastable fraction is found using a global model
- The pressure is varied from 10 – 500 mTorr

Capacitively Coupled Oxygen Discharge at 13.56 MHz

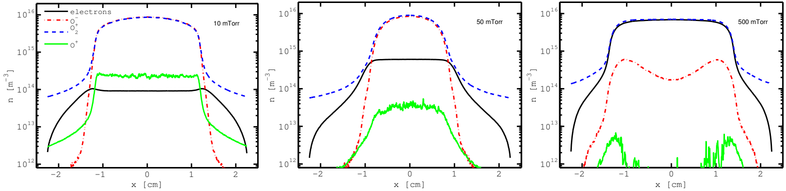

- For a parallel plate capacitively coupled oxygen discharge at 50 mTorr with with a gap separation of 4.5 cm by a 222 V voltage source at 13.56 MHz
  - O_2^+-ion density profile
  - O^+-ion density profile
  - O^--ion density profile
  - electron density profile

Gudmundsson and Ventéjou (2015) JAP **118** 153302

Capacitively Coupled Oxygen Discharge at 13.56 MHz

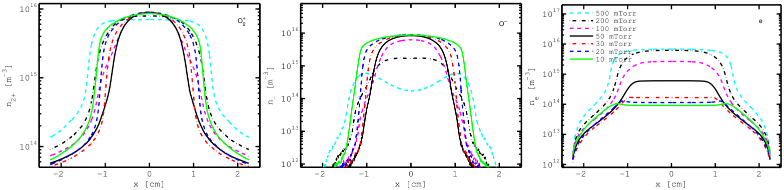

- The sheath width decreases as the pressure is decreased in the pressure range from 50 mTorr to 10 mTorr
- The sheath widths are largest at 50 mTorr
- As the pressure is increased from 50 mTorr up to 500 mTorr the sheath width decreases
- This agrees with what has been observed experimentally in the pressure range 40 – 375 mTorr

Mutsukura et al. (1990) JAP **68** 2657 and van Roosmalen et al. (1985) JAP **58** 653

Capacitively Coupled Oxygen Discharge at 13.56 MHz

- The electron heating profile $\mathbf{J}_{\rm e} \cdot \mathbf{E}$
- In the pressure range 50 - 500 mTorr the electron heating occurs almost solely in the sheath region
- As the pressure is decreased the Ohmic heating contribution in the plasma bulk increases and sheath heating decreases

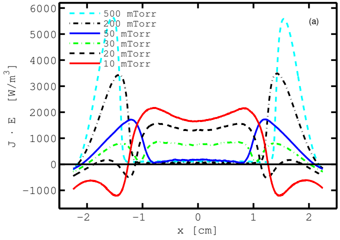

Gudmundsson and Ventéjou (2015) JAP **118** 153302

Capacitively Coupled Oxygen Discharge at 13.56 MHz

- At 10 mTorr excluding the metastable states in the simulation has very small influence on the heating mechanism
- At 50 mTorr the metastable states $O_2(a^1\Delta_g)$ have a significant influence on the heating mechanism
- The role of the metastables is even more significant at 200 mTorr

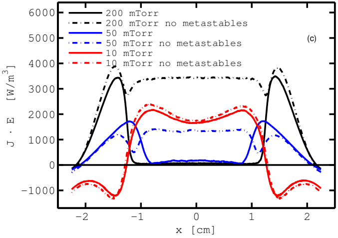

Gudmundsson and Ventéjou (2015) JAP **118** 153302

Gudmundsson and Lieberman (2015) PSST **24** 035016

Capacitively Coupled Oxygen Discharge at 13.56 MHz

- At low pressure the EEPF is convex, the population of low energy electrons is relatively low
- As the pressure is increased the number of low energy electrons increases and the number of higher energy electrons ($>$ 10 eV) decreases
- Thus the EEPF develops a concave shape or becomes bi-Maxwellian as the pressure is increased

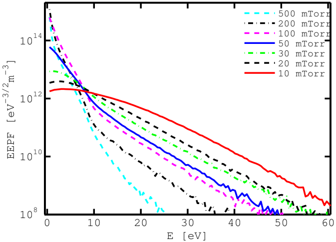

Gudmundsson and Ventéjou (2015) JAP **118** 153302

Capacitively Coupled Oxygen Discharge at 13.56 MHz

- Our results agree with the measurements of Lee et al. (2010) which explored experimentally the evolution of the EEPF with pressure in a capacitively coupled oxygen discharge in the pressure range 3 – 100 mTorr
- They find that the EEPF became more distinctly bi-Maxwellian and the density of low energy electrons increases as the gas pressure is increased

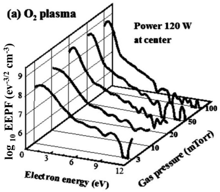

Lee et al. (2010) PRE **81** 046402

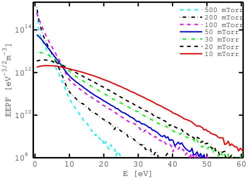

Gudmundsson and Ventéjou (2015) JAP **118** 153302

Capacitively Coupled Oxygen Discharge at 13.56 MHz

- The effective electron temperature drops as the pressure is increased
- We had seen earlier that when the metastable singlet oxygen molecule $O_2(a^1\Delta_g)$ is added to the discharge model the effective electron temperature drops, in particular in the electronegative core due to detachment by the metastable $O_2(a^1\Delta_g)$ molecule

$$O^- + O_2(a^1\Delta_g) \rightarrow \text{products}$$

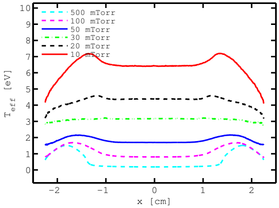

Gudmundsson and Ventéjou (2015) JAP **118** 153302

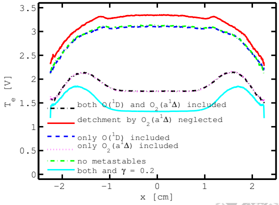

Gudmundsson and Lieberman (2015) PSST **24** 035016

Capacitively Coupled Oxygen Discharge at 13.56 MHz

- At low pressure the EEPF is convex and develops a concave shape or becomes bi-Maxwellian as the pressure is increased
- These results contradict what is commonly found for the capacitively coupled argon discharge where the EEPF evolves from being concave at low pressure to being convex at high pressure

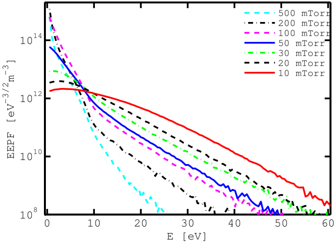

Gudmundsson and Ventéjou (2015) JAP **118** 153302

B.2. The chlorine discharge

The chlorine discharge

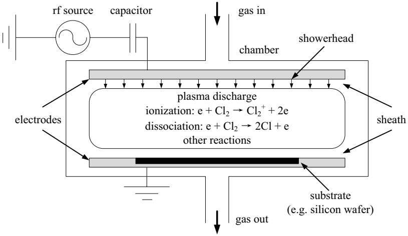

- We consider a discharge that consists of:
  - electrons
  - the ground state chlorine molecule $\mathrm{Cl}_2(X\,^1\Sigma_g^+, v=0)$,
  - the ground state chlorine atom $\mathrm{Cl}(3\mathrm{p}^5\,^2\mathrm{P})$
  - the negative chlorine ion Cl^-
  - the positive chlorine ions Cl^+ and Cl_2^+

The chlorine discharge

- In the chlorine discharge, the number of Cl atoms is much larger than the number of charged species
- Thus, we apply a global model[1] beforehand to calculate the fraction of Cl atoms under certain control parameters including the discharge pressure, absorbed power and the gap length between two electrodes
- The absorbed power found in the PIC/MCC simulation is used as an input parameter in the global model iteratively
- Both Cl_2 molecules and Cl atoms are treated as the initial background gas in the simulation

[1] Thorsteinsson and Gudmundsson, *Plasma Sources Sci. Technol.*, **19** 015001 (2010)

The chlorine discharge

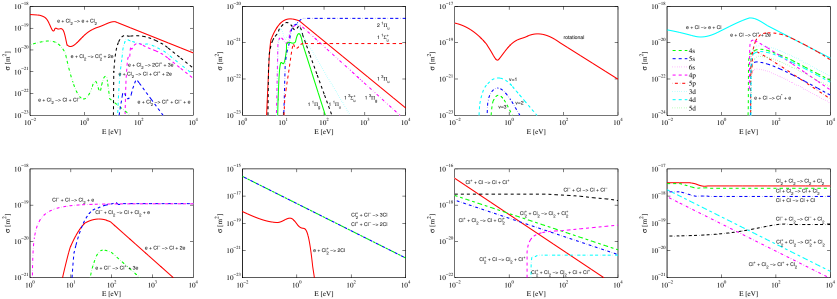

- The reaction set for the chlorine is comprehensive and includes 44 reactions

Huang and Gudmundsson, *Plasma Sources Sci. Technol.*, **22** 055020 (2013)

B.2.1 Capacitively Coupled Chlorine Discharge – dual frequency 27.12 MHz and 2 MHz – Current Source

Capacitively Coupled Chlorine Discharge at 27.12 MHz + 2 MHz

- We apply a current source that consists of two frequency components

$$J(t) = J_{\mathrm{hf}} \sin(2\pi f_{\mathrm{hf}} t) + J_{\mathrm{lf}} \sin(2\pi f_{\mathrm{lf}} t)$$

- The electrodes are circular with a diameter of 10.2 cm
- The gap between the electrodes is 2.54 cm
- We set J_{hf} = 40 A/m^2 and f = 27.12 MHz
- We set J_{lf} = 1 – 4 A/m^2 and f = 2 MHz
- The neutrals (Cl_2 and Cl) are treated as background gas at T_{g} = 300 K with a Maxwellian distribution
- The dissociation fraction is found using a global model
- The pressure is 10 mTorr

Huang and Gudmundsson, *Plasma Sources Sci. Technol.*, **23** (2014) 025015

Capacitively Coupled Chlorine Discharge at 27.12 MHz + 2 MHz

- In dual frequency CCP
  - the low frequency (LF) source is expected to predominantly control the ion energy distribution (IED) and the ion angular distribution (IAD)
  - the high frequency (HF) source should determine the ion flux to the substrate

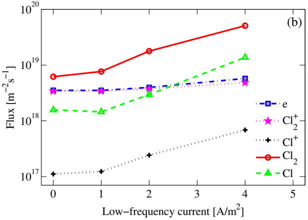

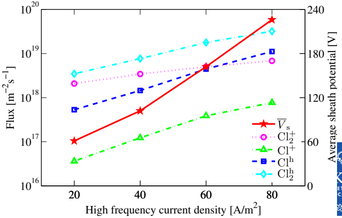

Capacitively Coupled Chlorine Discharge at 27.12 MHz + 2 MHz

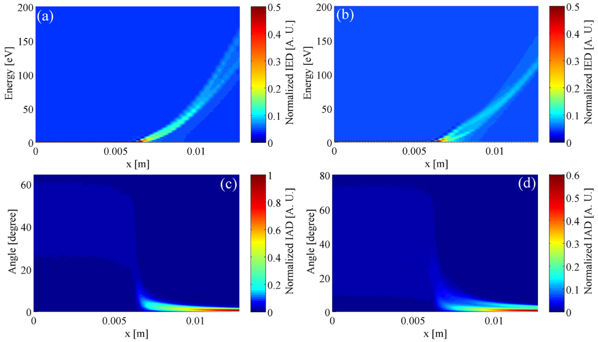

- As the ions reach the presheath–sheath boundary they are accelerated across the sheath towards the electrode
- The IEDs become wider and shift from single-peak to bimodal profile

Huang and Gudmundsson, *IEEE Trans. Plasma Science*, **42** (2014) 2854

Capacitively Coupled Chlorine Discharge at 27.12 MHz + 2 MHz

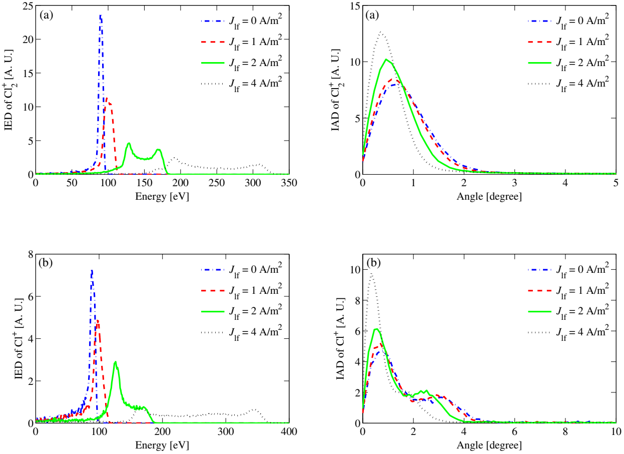

Huang and Gudmundsson, *Plasma Sources Sci. Technol.*, **24** 015003 (2015)

Capacitively Coupled Chlorine Discharge at 27.12 MHz + 2 MHz

- The IED becomes wider and extends to the high-energy region with increasing low-frequency current
- The IAD is more concentrated in the small-angle region with increasing low-frequency current

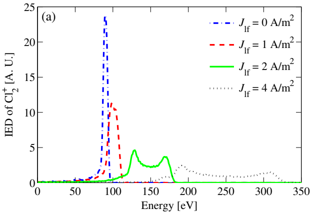

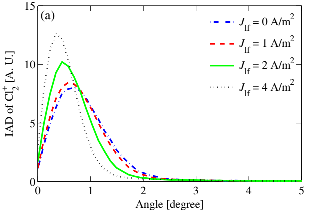

Summary

- We demonstrated particle-in-cell/Monte Carlo collision simulation of a capcacitively coupled disharge
- In an oxygen discharge at low pressure the EEPF is convex and develops a concave shape or becomes bi-Maxwellian as the pressure is increased
- These results contradict what is commonly found for the capacitively coupled argon discharge where the EEPF evolves from being concave at low pressure to being convex at high pressure
- In dual frequency discharge increased low frequency current leads to higher ion bombarding energy and decreases the angular spread of the ions

C. Overall Summary

Overall Summary

- A global (volume averaged) model can be used to understand the plasma chemistry
  - Which particles are important
  - Which reactions are important
  - How do the plasma parameters scale with the control parameters – power, pressure, discharge dimensions
- Particle-in-cell/Monte Carlo collision simulations can be used to explore the plasma kinetics
  - To find the electron energy distribution function
  - To find the ion energy distribution (IED) and the ion angular distribution (IAD)

Acknowledgements

The slides can be downloaded at

`http://langmuir.raunvis.hi.is/~tumi/ranns.html`

Much of this work was made by

- Eyþór Gísli Þorsteinsson (Univ. of Iceland)
- Shuo Huang (UM-SJTU, Shanghai)
- Aron Þór Hjartarson (Univ. of Iceland)
- Hólmfríður Hannesdóttir (Univ. of Iceland)
- Bruno Ventéjou (Université Paris Sud)
- David A. Toneli (Institute of Aeronautics, São José dos Campos)

in collaboration with

- prof. Michael A. Lieberman (UC Berkeley)
- prof. Allan J. Lichtenberg (UC Berkeley)
- prof. John P. Verboncoeur (Michigan State)
- Dr. Emi Kawamura (UC Berkeley)

and funded by Icelandic Research Fund grants no. 130029 and the Swedish Government Agency for Innovation Systems (VINNOVA) contract no. 2014-04876

References

Donnelly, V. M. and M. V. Malyshev (2000). Diagnostics of inductively coupled chlorine plasmas: Measurements of the neutral gas temperature. *Applied Physics Letters 77*(16), 2467–2469.

Godyak, V. A. (1986). *Soviet Radio Frequency Discharge Research*. Falls Church VA: Delphic Associates.

Gudmundsson, J. T. (2001). On the effect of the electron energy distribution on the plasma parameters of argon discharge: A global (volume averaged) model study. *Plasma Sources Science and Technology 10*(1), 76–81.

Gudmundsson, J. T. and E. G. Thorsteinsson (2007). Oxygen discharges diluted with argon: dissociation processes. *Plasma Sources Science and Technology 16*(2), 399–412.

Gudmundsson, J. T. and M. A. Lieberman (2015). On the role of metastables in capacitively coupled oxygen discharges. *Plasma Sources Science and Technology 24*(3), 035016.

Gudmundsson, J. T., A. T. Hjartarson, and E. G. Thorsteinsson (2012). The influence of the electron energy distribution on the low pressure chlorine discharge. *Vacuum 86*(7), 808–812.

Gudmundsson, J. T., E. Kawamura, and M. A. Lieberman (2013). A benchmark study of a capacitively coupled oxygen discharge of the oopd1 particle-in-cell Monte Carlo code. *Plasma Sources Science and Technology 22*(3), 035011.

Gudmundsson, J. T. and B. Ventéjou (2015). The pressure dependence of the discharge properties in a capacitively coupled oxygen discharge. *Journal of Applied Physics 118*(15), 153302.

Guha, J., V. M. Donnelly, and Y.-K. Pu (2008). Mass and Auger electron spectroscopy studies of the interactions of atomic and molecular chlorine on a plasma reactor wall. *Journal of Applied Physics 103*(1), 013306.

Hjartarson, A. T., E. G. Thorsteinsson, and J. T. Gudmundsson (2010). Low pressure hydrogen discharges diluted with argon explored using a global model. *Plasma Sources Science and Technology 19*(6), 065008.

Huang, S. and J. T. Gudmundsson (2013). A particle-in-cell/Monte Carlo simulation of a capacitively coupled chlorine discharge. *Plasma Sources Science and Technology 22*(5), 055020.

Huang, S. and J. T. Gudmundsson (2014). Ion energy and angular distributions in a dual-frequency capacitively coupled chlorine discharge. *IEEE Transactions on Plasma Science*, *42*(10), 2854.

Huang, S. and J. T. Gudmundsson (2014). A current driven capacitively coupled chlorine discharge. *Plasma Sources Science and Technology*, *23*(2), 025015.

Huang, S. and J. T. Gudmundsson (2015). Dual-frequency capacitively coupled chlorine discharge. *Plasma Sources Science and Technology*, *24*(1), 015003.

References

Kim, S., M. A. Lieberman, A. J. Lichtenberg, and J. T. Gudmundsson (2006). Improved volume-averaged model for steady and pulsed-power electronegative discharges. *Journal of Vacuum Science and Technology A 24*(6), 2025–2040.

Lee, M.-H., H.-C. Lee, and C.-W. Chung (2010). Comparison of pressure dependence of electron energy distributions in oxygen capacitively and inductively coupled plasmas. *Physical Review E 81*(4), 046402.

Lee, C. and M. A. Lieberman (1995). Global model of Ar, O_2, Cl_2 and Ar/O_2 high-density plasma discharges. *Journal of Vacuum Science and Technology A 13*(2), 368–380.

Lieberman, M. A. and A. J. Lichtenberg (2005). *Principles of Plasma Discharges and Materials Processing* (2 ed.). New York: John Wiley & Sons.

Malyshev, M. V. and V. M. Donnelly (2000). Diagnostics of inductively coupled chlorine plasmas: Measurement of Cl_2 and Cl number densities. *Journal of Applied Physics 88*(11), 6207 – 6215.

Malyshev, M. V. and V. M. Donnelly (2001). Diagnostics of inductively coupled chlorine plasmas: Measurement of electron and total positive ion densities. *Journal of Applied Physics 90*(3), 1130–1137.

Mutsukura, N., K. Kobayashi, and Y. Machi (1990). Plasma sheath thickness in radio-frequency discharges. *Journal of Applied Physics 68*(6), 2657–2660.

Stafford, L., R. Khare, J. Guha, V. M. Donnelly, J.-S. Poirier, and J. Margot (2009). Recombination of chlorine atoms on plasma-conditioned stainless steel surfaces in the presence of adsorbed Cl_2. *Journal of Physics D: Applied Physics 42*(5), 055206.

Thompson, J. B. (1961). The ion balance of the oxygen d.c. glow discharge. *Proceedings of the Royal Society A 262*(1311), 519–528.

Thorsteinsson, E. G. and J. T. Gudmundsson (2010a). A global (volume averaged) model of a chlorine discharge. *Plasma Sources Science and Technology 19*(1), 015001.

Thorsteinsson, E. G. and J. T. Gudmundsson (2010b). The low pressure Cl_2/O_2 discharge and the role of ClO. *Plasma Sources Science and Technology 19*(5), 055008.

Toneli, D. A., R. S. Pessoa, M. Roberto, and J. T. Gudmundsson (2015). On the formation and annihilation of the singlet molecular metastables in an oxygen discharge. *Journal of Physics D: Applied Physics 48*(32), 325202.

van Roosmalen, A. J., W. G. M. van den Hoek, and H. Kalter (1985). Electrical properties of planar rf discharges for dry etching. *Journal of Applied Physics 58*(2), 653–658.